Electronic structure and magnetic properties of Y-Fe compounds

R. F. Sabiryanov and S. S. Jaswal
Center for Materials Research and Analysis and Department of Physics and Astronomy, University of Nebraska, Lincoln, Nebraska 68588-0111
(Received 11 September 1997)

A low concentration of rare earths (R) plays an important role in magnetic materials because of their large anisotropy. However, the Curie temperature (T_C) has a decreasing trend with increasing Fe concentration in R-Fe compounds. In order to understand the variation of T_C as a function of iron concentration we carry out self-consistent spin-polarized electronic structure calculations for the sequence $YFe_2 \rightarrow YFe_3 \rightarrow Y_2Fe_{17} \rightarrow YFe_{12}$ where yttrium is a prototype R element. The exchange interaction parameters are derived using the infinitesimal angle approach. The Monte Carlo simulations based on the Heisenberg Hamiltonian are carried out to derive T_C of Y-Fe compounds and results are in very good agreement with experimental data. The changes in the magnetic properties with Fe concentration are analyzed in terms of the local environment and magnetovolume effects. [S0163-1829(98)01014-5]

I. INTRODUCTION

Rare-earth-iron (R-Fe) compounds have Curie temperatures (T_C) considerably lower than that of the bcc Fe and the T_C tends to decrease as the Fe concentration increases in these compounds.[1] The aim of this paper is to study this somewhat unusual behavior of T_C due to the structural changes with the increase in the Fe content. Analysis of the exchange interactions in crystalline bcc and fcc iron shows that they are long range in nature.[2] The effect of remote shells is especially strong in the fcc phase. This close-packed phase also has a strong magnetovolume effect. A similar behavior is expected for the iron-rich R-Fe compounds where the presence of R drives these systems to more close-packed structures. Recently we carried out first-principles T_C calculations in one of these compounds with results in very good agreement with the experimental data.[3] This work is extended here to study the trends in T_C for the sequence $YFe_2 \rightarrow YFe_3 \rightarrow Y_2Fe_{17} \rightarrow YFe_{12}$, where Y is a prototype R.

Electronic structure and magnetic properties (such as magnetization, distribution of local magnetic moments and magnetocrystalline anisotropy) of rare-earth–transition-metal compounds were studied from first principles in the local-density approximations during the last decade.[4–6] These studies show that this procedure works well for ground-state properties of R-Fe compounds. Coehoorn[7] gave elaborate analysis of the crystal and electronic structure of Y-Fe compounds. In this paper, self-consistent spin-polarized electronic structure calculations are performed for Y-Fe compounds (where Y is a prototype R). The exchange interaction parameters in the Heisenberg model are calculated using infinitesimal rotation approach. Monte Carlo simulations based on the Heisenberg model and finite-size scaling are carried out to calculate the Curie temperature in these complex materials.

II. COMPUTATIONAL PROCEDURE

The self-consistent spin-polarized linear muffin-tin orbitals (LMTO) method[8] is used to calculate the local spin-up and spin-down densities of states (DOS) and magnetic moments for Y-Fe compounds. The Heisenberg Hamiltonian is used to express exchange interactions as follows:

$$H_{\mathrm{ex}} = -\sum_{ij} J_{ij} \vec{e}_i \cdot \vec{e}_j , \tag{1}$$

where J_{ij} is the exchange-interaction parameter between sites i and j and $\vec{e}_i$ is the unit vector in the spin direction at site i. A method to calculate J_{ij}, based on the local approximation to spin-density functional theory, has been developed by Liechtenstein *et al.*[9] (A comprehensive review of different approaches to this problem has been provided by Gubanov *et al.*[10].) The change in the energy due to the rotation of one spin or two spins from the ground-state collinear in all magnetic moments can be put in an analytic form using the multiple-scattering formalism. Using spherical charge and spin densities and a local force theorem it is shown in Ref. 9 that

$$J_{ij} = \frac{1}{4\pi} \sum_{LL'} \mathrm{Im} \int_{-\infty}^{\varepsilon_F} d\varepsilon \Delta_l^i(\varepsilon) T_{LL'}^{ij\uparrow}(\varepsilon) \Delta_{l'}^j(\varepsilon) T_{LL'}^{ij\downarrow}(\varepsilon). \tag{2}$$

Here $T_{LL'}^{ij\sigma}$ is the scattering path operator in the site (i,j) representation for different spin projections ($\sigma = \uparrow, \downarrow$), and $\Delta_l^i(\varepsilon) = t_{i\uparrow}^{-1} - t_{i\downarrow}^{-1}$ is the difference of the inverse single-site scattering matrices.

The total exchange interaction of the given site 0 with all the other sites i,

$$J_0 = \sum_{i \neq 0} J_{0i}, \tag{3}$$

can also be calculated from the relation[9]

$$J_0 = -\frac{1}{4\pi} \sum_{LL'} \mathrm{Im} \int_{-\infty}^{\varepsilon_F} d\varepsilon \{\Delta_l^0(\varepsilon)[T_{LL'}^{00\uparrow}(\varepsilon) - T_{LL'}^{00\downarrow}(\varepsilon)] + \Delta_l^0(\varepsilon) T_{LL'}^{00\uparrow}(\varepsilon) \Delta_{l'}^0(\varepsilon) T_{LL'}^{00\downarrow}(\varepsilon)\}. \tag{4}$$

TABLE I. Number of k points in the irreducible wedge of the Brillouin zone, Fe Wigner-Seitz radii (R_{WS}), and supercell size (the number of sites) in Monte Carlo calculations for Y-Fe compounds.

	YFe_2	YFe_3	Y_2Fe_{17}	YFe_{12}
Number of k points	176	288	288	163
R_{WS}	2.623	2.641	2.641	2.668
	1 000	1 125	2 125	2 592
Supercell	2 744	3 087	5 831	6 144
Sizes (N)	8 000	9 000	8 704	12 000
	10 648	11 979		

The procedure to calculate $T_{LL'}^{ij\sigma}$ in the LMTO formalism has been developed by Gunnarsson *et al.*[11] Following Coehoorn[7] we set the ratio between the Wigner-Seitz radii of yttrium and iron equal to 1.35. The number of k points used and the Wigner-Seitz radii of Fe atoms in various compounds are listed in Table I. Integration is performed in the complex plane over the elliptical contour using Gaussian quadrature procedure. The exchange parameters were calculated for all neighbors inside the 5.5 Å distance around a given site. A larger cutoff distance is beyond our present computational power due to the dramatic increase in the number of neighbors.

The Heisenberg Hamiltonian [Eq. (1)] is used in the Monte Carlo simulations for T_C calculations. The Metropolis algorithm[12] is employed to find the thermodynamic averages of M^n for $n=1-4$ as a function of temperature for the cell sizes listed in Table I, where M is the magnetization. The T_C for each cell is calculated from the location of the extrema of the thermodynamic quantities such as susceptibility and third- and fourth-order cumulants, following a procedure proposed by Chen *et al.*[13] The extremum values as a function of the cell size N follows the scaling law:

$$T_C(N) \approx T_c + a_q N^{-1/3\nu}, \tag{5}$$

where a_q is a thermodynamic quantity-dependent constant and ν is a critical exponent. For the correct value of ν, $T_C(N)$ plotted as a function of $N^{-1/3\nu}$ is a straight line with the intercept as the T_C for the infinite size of the cell.

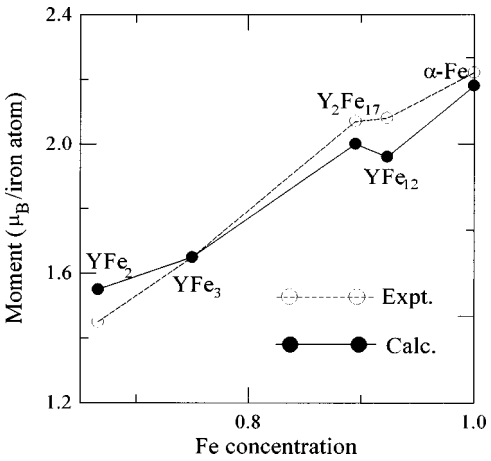

FIG. 1. Magnetization as a function of the Fe concentration. The experimental data are from Ref. 7.

III. RESULTS AND DISCUSSION

The changes in the magnetic properties of Y-Fe compounds as a function of the Fe concentration depend on the chemical composition and the crystal structure. Crystallographic data for Y-Fe compounds can be found in *Pearson's Handbook*[14] and they are summarized by Coehoorn.[7] The distribution of local magnetic moments is presented in Table II. The dependence of magnetization on the iron concentration is presented in Fig. 1. Our results are similar to those of Coehoorn.[7]

We first consider briefly the effect of the Y atoms on the electronic structure and magnetization of Y-Fe compounds. Due to the size difference between the Y and Fe atoms the former has a large number of neighbors (~ 20). As a result, the individual hybridization of a Y-Fe pair is not very strong because Y has to ''share'' its valence electrons with all Fe and Y neighbors. However, the Y-Fe hybridization causes

TABLE II. Numbers of first neighbors (m), Voronoi polyhedron volumes (V), exchange parameters (J_0), magnetic moments (M_i) of Fe atoms and Curie temperatures of yttrium-iron compounds.

		m (all/Fe)	V	J_0^d (meV)	M_i (μ_B)	T_C (calc.) (K)	T_C(expt.) (K)
YFe_2	1Fe(d)	12/6	12.21	105(108)	1.89	650	570[a]
YFe_3	1Fe(b)	12/6	13.64	120(96)	1.73	592	580[a]
	2Fe(c)	12/9	13.95	133(116)	2.10		
	6Fe(h)	12/7	13.83	96(92)	1.77		
Y_2Fe_{17}	2Fe(c)	14/13	14.02	73(97)	2.51	262	300[b]
	3Fe(d)	12/10	12.67	67(64)	1.50		
	6Fe(f)	12/10	13.47	30(47)	2.10		
	6Fe(h)	12/9	13.78	11(32)	2.10		
YFe_{12}	4Fe(j)	12/10	11.21	79(78)	1.55	486	$\approx$500[c]
	4Fe(i)	14/13	12.60	125(101)	2.33		
	4Fe(f)	12/10	11.86	48(61)	2.09		

[a]Reference 15.
[b]Reference 16.
[c]An extrapolated value of T_C from Ref. 17 for the hypothetical structure YFe_{12}.
[d]First and second number are obtained from Eqs. (4) and (3), respectively.

the deviation from the rigid band behavior of Fe states because Y atoms, being nonmagnetic, have different hybridization with minority and majority spins. Since the Y states hybridize more with the minority states, they develop small magnetic moments, opposite to those of the Fe atoms. Finally, the Y atom tends to lower the magnetic moment of a neighboring Fe atoms through this hybridization.

The rest of this section deals with the analysis of the magnetic properties and exchange interactions in terms of the local environment of iron atoms in these compounds. To characterize the structure from the standpoint of local environment one can employ parameters describing the local symmetry of the atomic configuration such as volumes V and the number of faces (f) of Voronoi polyhedra (VP). The magnetovolume effect is qualitatively reflected in the VP volumes of different Fe sites in a given compound. The quantity f gives the number of first neighbors which determine the strength of the hybridization. Fe atoms in Y-Fe compounds have 12–14 first neighbors (the neighbors which give rise to the faces of the Voronoi polyhedron) as can be seen from Table II. But the number of Fe first neighbors and the Fe-Fe interatomic distances among them vary considerably. (Tables II and III).

In YFe_2 compound (Laves phase) each Fe atom has six nearest-neighbor Fe atoms. Iron sublattice forms a network of connected tetrahedra. Six Y atoms form a second-neighbor shell (with bond length ~ 1.15 of Fe-Fe nearest-neighbor bond length) and 12 iron atoms are in the third shell of neighbors at a distance which would correspond to the third neighbors in fcc iron (fcc iron has 48 third neighbors). Thus, each iron atom has fewer neighbors than close-packed structures and the second shell is formed by nonmagnetic atoms. As a result, Fe density of states (DOS) in YFe_2 (Fig. 2) has quite narrow d band with sharp peaks in the majority DOS about 1 eV below the Fermi energy. The exchange splitting and the magnetic moment are smaller in YFe_2 than in bcc Fe because of the hybridization of primarily the minority Fe d states with the neighboring Y states.

YFe_3 has rhombohedral structure and three inequivalent iron sites. The c site has the largest magnetic moment and the most narrow peaks of the DOS (Fig. 3) among all three sites because it has the largest VP volume and the lowest number of Y neighbors. The b site is similar to c, but due to the hybridization of the minority d electrons with the additional Y neighbors (which increases the occupation of the minority states) and also partially due to slightly smaller volume, its magnetic moment is smaller than that of the c site. h site moment is similar to that of the b site but its local environment is more complex than either of the other two sites as reflected in the DOS and J_0 value.

Y_2Fe_{17} has rhombohedral structure and can be obtained from YFe_5 by replacing one third of the Y atoms by Fe pairs (dumbbells). Because of its structural similarity to fcc phase, the magnetic properties of Y_2Fe_{17} share some features with fcc Fe. For example, both phases have strong magnetovolume effect. However, Y_2Fe_{17} has four inequivalent Fe sites where c site has the largest volume and the largest number of first neighbors among Fe sites, while d site has the smallest volume. Thus, we have not only the global but also the local volume effect in this compound with the magnetic moments ranging from $2.5\mu_B$ for the c site to $1.5\mu_B$ for the d site. The presence of three Y atoms in the second shell of the d site also decreases its moment. c and d sites also have the least uniform local environment from the point of view of spatial position of the neighbors and interatomic distances. The c site has one neighbor at a very short distance, while the d site has quite a variation of distances which makes this site less similar to the close-packed environment among all the sites. The DOS (Fig. 4) of site c has the narrowest peaks, while other sites have broader peaks. We also see the rigid-band-type shift of the majority states to the higher energy from the c to d site with f and h sites having intermediate positions of DOS peaks.

Y in YFe_{12} can be imagined as an impurity in the Fe host (7.6 at. %). However, the Y atom changes considerably the environment of Fe atoms due to its large size. f and j sites have ten iron first neighbors and two Y atoms in the second shell (somewhat similar to the fcc structure). The i site is completely different: it has a very close i site, and the rest of the first neighbors split into two subshells of eight and four iron atoms (Table III). This site also has three 4- and 6-edge faces making it closer to the bcc Fe phase. The difference in the local environment is reflected in the DOS (Fig. 5) and the magnitudes of the magnetic moments.

The change in the number of first-neighbor iron atoms effects considerably the magnetic properties of these compounds. For a low first-neighbor compound (YFe_2 and YFe_3 with 6–8 neighbors) the DOS is narrower and peaks are sharper than a high first-neighbor compound and the Fermi energy (E_F) is not located next to any major peak in DOS. Therefore, like bcc Fe, such a system is not expected to show any appreciable magnetovolume effect. On the other hand, a high first-neighbor compound (Y_2Fe_{17}) has the Fermi energy on the sharp slope of the large peak in the majority DOS and this, as in the case of fcc iron, is responsible for the well-known large magnetovolume effect in this system. YFe_{12} has a mixture of two ''close-packed'' sites and a more open i site. As a result, the magnetovolume effect in this system is less pronounced than that in Y_2Fe_{17}.

Next we consider the exchange interactions J_{ij} among Fe pairs needed in the Heisenberg Hamiltonian for the T_C calculations (Table III). It is clear from the table that the exchange interactions are fairly long range for all the compounds being studied here. The dumbbell exchange interactions in Y_2Fe_{17} are strongly ferromagnetic which is contrary to the occasional speculation that they are antiferromagnetic. We consider the agreement between J_0s calculated from the pair interactions [Eq. (3)] and the exact results calculated directly from Eq. (4) reasonable as shown in Table II within the constraint of our computational facilities.

Due to the oscillatory and decaying nature of J_{ij}, the largest contribution to J_0 comes from the first neighbors. The average values of the sum of the first-neighbor exchange interactions over inequivalent Fe sites ($\langle J_{01} \rangle$) for YFe_2, YFe_3, Y_2Fe_{17}, and YFe_{12} are 91, 77, 52, and 81 meV, respectively. The value of $\langle J_{01} \rangle$ is effected by the number of the first-neighbor Fe atoms and their distribution. In general, an increase in the first-neighbor Fe atoms randomizes their distribution into a broad group which leads to a decrease in $\langle J_{01} \rangle$. However, in the case of YFe_{12}, the first-neighbor group breaks up into two distinct subshells for the site i similar to bcc iron which leads to a very large value of its

TABLE III. Fe-Fe pair-exchange parameters (meV) for three shells in Y-Fe compounds. The numbers in the brackets are the number of neighbors and their distance (Å), respectively.

		J_{01}	J_{02}	J_{03}
YFe_2	Fe(d)	15.2(6×2.604)	1.14(12×4.509)	1.34(12×5.206)
YFe_3	Fe(b)	11.9(6×2.560)	1.37(2×4.074)	2.39(6×5.080)
			0.87(12×4.442)	−0.046(6×5.133)
	Fe(c)	9.7(3×2.478)	1.37(1×4.074)	2.39(3×5.080)
		11.7(3×2.520)	−1.01(6×4.395)	−0.03(6×5.133)
		18.8(3×2.963)	−1.06(6×4.418)	
	Fe(h)	9.7(1×2.478)	−0.03(1×4.025)	−0.84(4×4.773)
		11.7(1×2.520)	−1.01(2×4.395)	−0.68(3×5.120)
		11.9(1×2.560)	−1.06(2×4.418)	5.80(6×5.133)
		7.5(4×2.567)	1.21(2×4.431)	
			0.87(2×4.442)	
			0.23(4×4.445)	
Y_2Fe_{17}	Fe(c)	62.1(1×2.355)	1.44(3×4.043)	1.21(3×5.183)
		2.1(3×2.591)	−0.39(3×4.140)	1.10(6×5.237)
		7.6(3×2.622)	−0.52(6×4.202)	−0.63(3×5.413)
		3.6(6×2.706)	−2.28(6×4.293)	
	Fe(d)	7.2(4×2.403)	0.69(4×4.010)	0.39(4×4.653)
		4.3(4×2.436)	1.44(2×4.043)	2.11(4×4.761)
		2.1(2×2.591)	−0.13(2×4.223)	−0.88(2×4.867)
			−0.37(4×4.230)	2.38(4×4.895)
			0.03(4×4.577)	−1.34(4×5.137)
	Fe(f)	7.2(2×2.403)	6.23(1×3.587)	−1.64(2×4.650)
		12.4(2×2.436)	0.69(2×4.010)	5.12(2×4.806)
		4.0(2×2.516)	−1.92(2×4.069)	0.72(1×4.873)
		−2.4(2×2.620)	0.81(2×4.134)	3.88(4×5.089)
		3.6(2×2.706)	−3.69(2×4.142)	−1.34(2×5.137)
			−0.09(2×4.153)	−1.55(2×5.175)
			−0.52(2×4.202)	−0.52(4×5.248)
			−3.83(2×4.220)	
			0.03(2×4.577)	
	Fe(h)	4.3(2×2.436)	5.28(1×3.819)	−1.64(2×4.650)
		8.3(2×2.476)	−1.92(2×4.069)	0.39(2×4.653)
		4.0(2×2.516)	0.81(2×4.134)	−1.94(4×4.763)
		−2.4(2×2.620)	−0.39(1×4.140)	−0.88(2×4.867)
		7.6(1×2.622)	−0.09(2×4.153)	3.94(1×4.873)
			0.84(2×4.196)	2.38(2×4.895)
			−0.13(1×4.223)	−2.87(2×4.930)
			3.42(2×4.264)	1.75(2×4.986)
			−2.28(2×4.293)	−1.55(2×5.165)
YFe_{12}	Fe(j)	11.7(2×2.380)	0.05(4×4.102)	−0.64(4×4.678)
		9.8(4×2.439)	2.58(4×4.155)	−0.36(2×4.758)
		2.7(4×2.598)	3.04(4×4.233)	−0.10(8×4.856)
			−1.52(4×4.251)	0.07(4×5.083)
	Fe(i)	49.0(1×2.380)	0.05(4×4.102)	0.71(2×4.758)
		2.7(4×2.598)	−1.52(4×4.251)	−0.38(4×5.196)
		5.6(4×2.634)	−1.15(2×4.266)	3.43(2×5.230)
		10.3(4×2.915)	−1.17(2×4.288)	−0.64(4×5.452)
			−2.04(4×4.297)	−0.05(2×5.469)
			−2.66(2×4.306)	
	Fe(f)	9.8(4×2.439)	0.17(1×4.087)	−1.48(1×4.674)
		5.6(4×2.534)	2.58(4×4.155)	−0.64(2×4.678)
		−6.3(2×2.662)	−2.04(4×4.297)	0.38(4×4.758)
				0.44(2×4.876)
				0.07(2×5.083)
				3.43(4×5.230)
				−1.62(4×5.439)

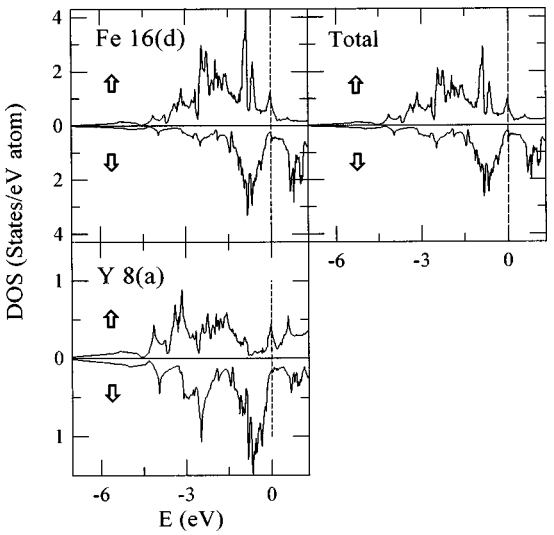

FIG. 2. Total and site-projected spin-polarized densities of states of YFe_2. The zero of the energy (E) corresponds to the Fermi energy.

J_{01}. This is the reason for the deviation for YFe_{12} from the decreasing trend of J_0 with increasing Fe concentration (Fig. 7).

The Heisenberg Hamiltonian calculated above is used in Monte Carlo simulations to find T_C of the Y-Fe compounds using the procedure outlined in Sec. II. An example of this procedure is presented in Fig. 6 for YFe_3, where susceptibility is plotted as a function of the temperature for different cell sizes in Fig. 6(a) and the location of the extrema of the

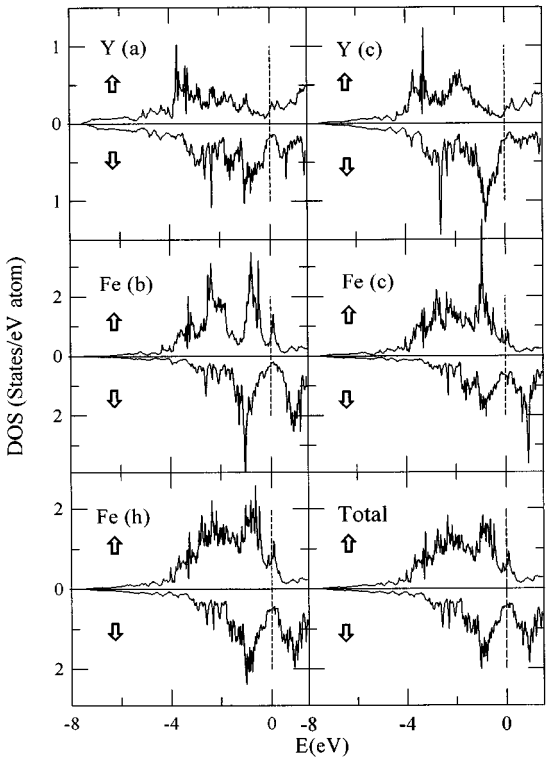

FIG. 3. Total and site-projected spin-polarized densities of states of YFe_3. The zero of the energy (E) corresponds to the Fermi energy.

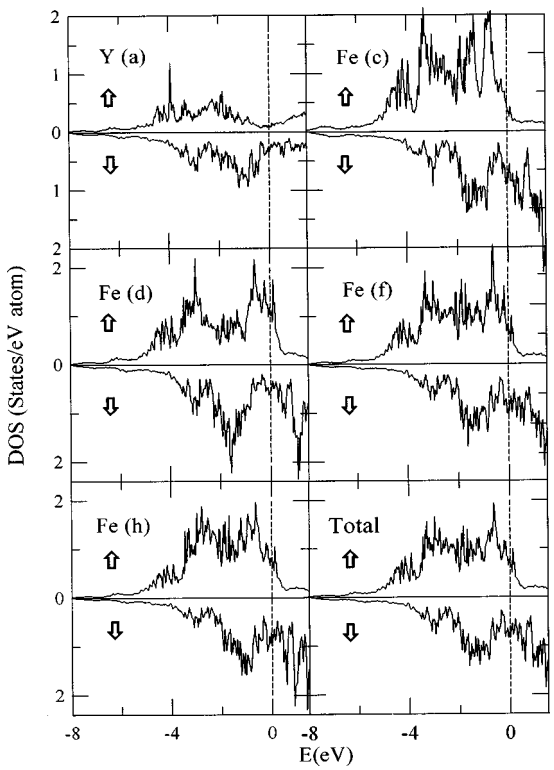

FIG. 4. Total and site-projected spin-polarized densities of states of Y_2Fe_{17}. The zero of the energy (E) corresponds to the Fermi energy.

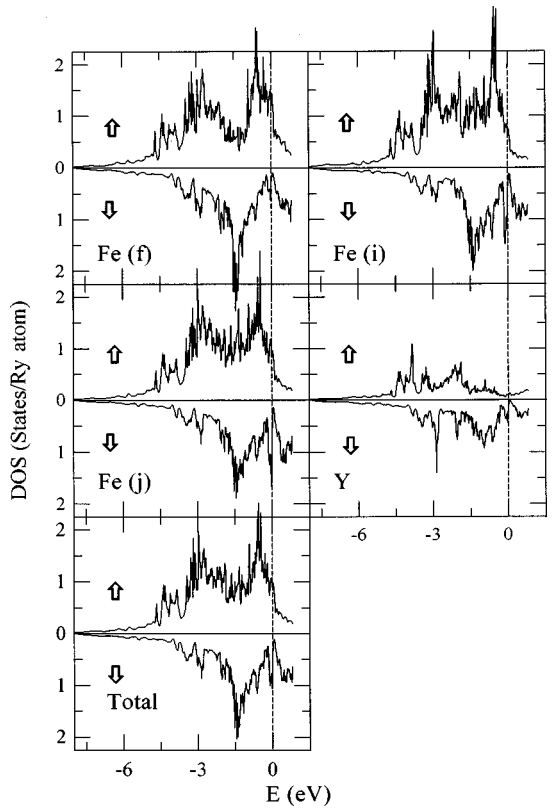

FIG. 5. Total and site-projected spin-polarized densities of states of YFe_{12}. The zero of the energy (E) corresponds to the Fermi energy.

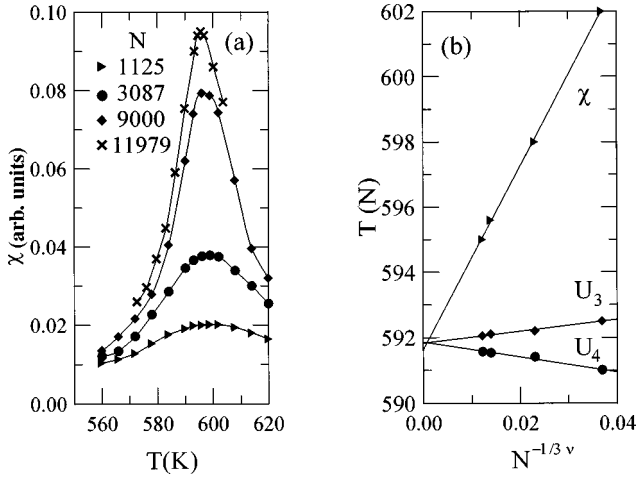

FIG. 6. Example of the finite-size scaling procedure for YFe_3: (a) Susceptibility (χ) as a function of the supercell size (N); (b) The location of the maxima of the thermodynamic quantities [susceptibility (χ), third- and fourth-order cumulants (U_3 and U_4)] as a function of $N^{-1/3\nu}$.

susceptibility and third and fourth cumulants are plotted as a functions of $N^{-1/3\nu}$ in Fig. 6(b). The straight line fits like those in Fig. 6(b) correspond to a value of $\nu=0.705$ and the intercepts give T_C for considered compound. The calculated values of T_C are in very good agreement with the experimental data as shown in Table II. According to the mean-field theory, $T_C \simeq 2/3 k_B \langle J_0 \rangle$ where $\langle J_0 \rangle$ is the average of $J_0(E_F)$ over different Fe sites. It is interesting to note that Monte Carlo values of T_C are proportional to $\langle J_0 \rangle$ (See Fig. 7) but the proportionality constant is about 0.76 of that of the mean-field value.

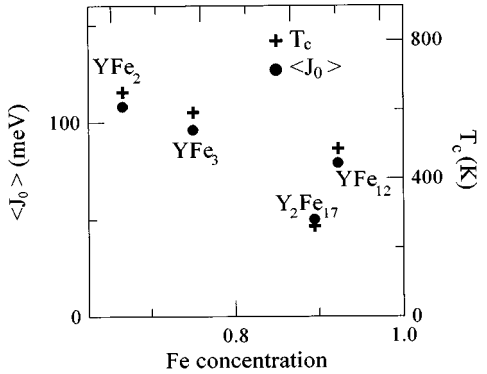

FIG. 7. Total exchange interaction averaged over inequivalent Fe sites ($\langle J_0 \rangle$) and calculated T_C as functions of the iron concentration in different Y-Fe compounds.

IV. CONCLUSIONS

Ab initio studies of the electronic structure and the magnetic properties of Y-Fe compounds are carried out and analyzed in terms of the local environment parameters such as the volume of the Voronoi polyhedron and the hybridization of a given atom with its neighbors. The exchange parameters calculated from the electronic structure have long-range oscillatory behavior with their values decreasing with distance. The first-neighbor interactions are strong for the low coordination sites and weak for the high coordination sites, where they become comparable with farther-neighbor interactions. The Curie temperatures calculated using the Monte Carlo procedure and the calculated exchange parameters are in very good agreement with the experimental data. The change in T_C with Fe concentration in Y-Fe compounds is strongly correlated with the first-neighbor Fe-Fe coordination and distribution. The Fe sites with bcc Fe-like first-neighbor two-subshell environments have larger exchange interactions than those with an amorphous distribution of the first neighbors. As a result, the Curie temperature tends to decrease with increasing iron concentration.

ACKNOWLEDGMENTS

This work was supported by the National Science Foundation under Grant Nos. DMR9705044 and OSR925525 and the U.S. Department of Energy under Grant No. DE-FG2-86ER45262.

[1] K. H. J. Buschow, Phys. Status Solidi A **7**, 199 (1971).
[2] R. F. Sabiryanov, S. K. Bose, and O. N. Mryasov, Phys. Rev. B **51**, 8958 (1995).
[3] R. F. Sabiryanov and S. S. Jaswal, Phys. Rev. Lett. **79**, 155 (1997).
[4] S. S. Jaswal, Phys. Rev. B **41**, 9697 (1990).
[5] S. S. Jaswal, W. B. Yelon, G. C. Hajipanayis, Y. Z. Wang, and D. J. Sellmyer, Phys. Rev. Lett. **67**, 644 (1991).
[6] S. S. Jaswal, Phys. Rev. B **48**, 6156 (1993).
[7] R. Coehoorn, Phys. Rev. B **39**, 13 072 (1989); R. Coehoorn, *ibid.* **41**, 11 790 (1990);
[8] O. K. Andersen, Phys. Rev. B **8**, 3060 (1975).
[9] A. I. Liechtenstein, M. I. Katsnelson, V. P. Antropov, and V. A. Gubanov, J. Magn. Magn. Mater. **21**, 35 (1988).
[10] V. A. Gubanov, A. I. Liechtenstein, and A. V. Postnikov, *Magnetism and the Electronic Structure of Crystals*, edited by M. Cardona, P. Fulde, K. von Klitzing, and H.-J. Queisser (Springer, Berlin, 1992).
[11] O. Gunnarsson, O. Jepsen, and O. K. Andersen, Phys. Rev. B **27**, 7144 (1983).
[12] N. Metropolis, A. W. Rosenbluth, M. N. Rosenbluth, A. H. Teller, and E. Teller, J. Chem. Phys. **21**, 1087 (1953).
[13] K. Chen, A. M. Ferrenberg, and D. P. Landau, Phys. Rev. B **48**, 3249 (1993).
[14] P. Villars and L. D. Calvert, *Pearson's Handbook of Crystallographic Data for Intermetallic Phases* (American Society of Metals, Metals Park, OH, 1985).
[15] J. P. Gavigan, D. Givord, H. S. Li, and J. Voiron, Physica B **149**, 345 (1988).
[16] H. Fujii, M. Akayama, K. Nakao, and K. Tatami, J. Alloys Compd. **219**, 10 (1995).
[17] H. Sun, M. Akayama, K. Tatami, and H. Fijii, Physica B **183**, 33 (1993).